IEEE Access
Multidisciplinary | Rapid Review | Open Access Journal

Received August 16, 2019, accepted September 12, 2019, date of publication September 18, 2019, date of current version October 2, 2019.

Digital Object Identifier 10.1109/ACCESS.2019.2942080

An Analysis Method of Oscillating Grinding Motion Model for Crankshaft Pin Journal

LIPING WANG[1], DONG WANG[1], BO WANG[1], AND WEIHUA LI[2]

[1]Department of Mechanical Engineering, Institute of Manufacturing Engineering, Tsinghua University, Beijing 100084, China
[2]Beier Machine Tool Works Company Ltd., Beijing 102444, China

Corresponding author: Dong Wang (dongwang2018@mail.tsinghua.edu.cn)

This work was supported in part by the National Postdoctoral Program for Innovative Talents under Grant BX20180166, and in part by the Science and Technology Major Project-Advanced NC Machine Tools & Basic Manufacturing Equipments under Grant 2016ZX04003-001.

ABSTRACT Oscillating grinding is a high-efficiency machining method for crankshaft pin journal, and motion model is one of the important foundations of oscillating grinding, which heavily affects the grinding quality. This paper proposes an analysis method of oscillating grinding motion model for crankshaft pin journal, which can provide an effective tool for engineers and technicians to quickly evaluate different motion models in practice. First, the method is described by performing characteristics analysis of oscillating grinding, including the velocity characteristics at grinding point and the performance of driving axis. A complete analysis flow is also given. Then, a numerical comparison example is given between two main oscillating grinding motion models, i.e. the constant linear velocity motion model (CLVMM) and the constant angular velocity motion model (CAVMM), and the results show that the CAVMM is more practical than the CLVMM by using the proposed method. Finally, a crankshaft pin journal grinding experiment is carried out on a prototype, and the result also indicates that the CAVMM is much better in practice, which validates the effectiveness of the proposed analysis method of oscillating grinding motion model.

INDEX TERMS Oscillating grinding motion model, crankshaft pin journal, velocity characteristics, performance of driving axis.

I. INTRODUCTION

Crankshaft is the most important component of automobile engine [1], [2], which bears impact load and transfers power. The machining quality of crankshaft heavily affects the performance and reliability of automobile engine, thus, the crankshaft manufacturing plays a very significant role in automotive industry. The manufacturing process of a crankshaft is complicated, and grinding is the last step to determine the dimensional accuracy of a crankshaft [3], [4]. A typical crankshaft with four cylinders [5] is shown in Fig. 1. One may see that the grinding of pin journal is non-circular, which is much harder than the grinding of main journal. Traditional grinding method of pin journal needs appropriative fixture, which leads to repeated position error and low machining efficiency.

In order to meet the accuracy and efficiency requirements in the mass production process of crankshafts, the oscillating grinding (aka. contour-controlled grinding) machine tool [6], [7] has been designed and developed. During the oscillating grinding process, the NC system controls the linkage between grinding carriage-axis and workpiece rotation-axis to ensure that the grinding wheel is always tangent with pin journal, which eliminates the repeated position error and improves the machining efficiency.

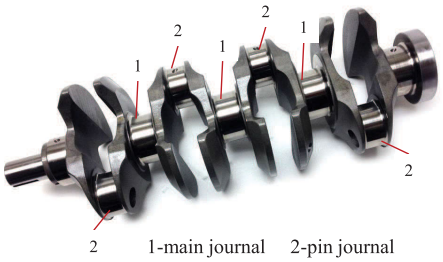

FIGURE 1. A crankshaft with four cylinders [5].

Some scholars have carried out related research of oscillating grinding for crankshaft pin journal. For example, an active tailstock is designed by Denkena and Gümmer [8], [9]; a grinding force prediction method is introduced by

The associate editor coordinating the review of this manuscript and approving it for publication was Wen-Sheng Zhao.

Walsh *et al.* [10]; an in-situ roundness measurement and correction method is studied by Yu *et al.* [11]; a research on the dynamic characteristics and stability of an oscillating grinding machine tool is performed by Cha *et al.* [12]; the thermal damage of non-circular grinding is researched by Krajnik *et al.* [13], [14]; a high efficient grinding strategy of pin journal is proposed by Comely *et al.* [15]; a surface roughness prediction study is performed by Torims *et al.* [16]; the optimum grinding velocity related to hardness is obtained by Fricker *et al.* [17]; a soft error compensation method of oscillating grinding machine tool is proposed by Liu *et al.* [18]. Overall, it should be pointed out that the open literature of oscillating grinding for crankshaft pin journal is very limited due to the huge commercial potential and value.

The motion model between grinding carriage-axis and workpiece rotation-axis is the important foundation of oscillating grinding [19], which will affect the grinding quality of crankshaft pin journal and the requirement of oscillating grinding machine tool. On the other hand, although the study on related technology of machine tool has been a hot topic [20]–[22], there is fewer research on the analysis method of oscillating grinding motion model. Thus, it has a great significance to establish a complete analysis method of oscillating grinding motion model, which should consider both theory and practice. Based on this point, the paper investigates an analysis method of oscillating grinding motion model for crankshaft pin journal. First, the characteristics analysis of oscillating grinding is performed, including the velocity characteristics at grinding point and the performance of driving axis, and the complete analysis flow is also given; then, a numerical comparison example between the constant linear velocity motion model (CLVMM) and the constant angular velocity motion model (CAVMM) is carried out based on the proposed analysis method; finally, a crankshaft grinding experiment is completed to validate the effectiveness of the proposed analysis method of oscillating grinding motion model.

The rest parts of the paper are organized as follows: Section 2 performs the characteristics analysis of oscillating grinding; Section 3 gives a numerical comparison example between two oscillating grinding motion models; Section 4 performs the crankshaft pin journal grinding experiment; Section 5 states the conclusion.

II. CHARACTERISTICS ANALYSIS OF OSCILLATING GRINDING

In this section, the basic relations of oscillating grinding are firstly given; then, the characteristics analysis of oscillating grinding will be performed, including the velocity characteristics at grinding point and the performance of driving axis.

A. BASIC RELATIONS OF OSCILLATING GRINDING

As shown in Fig. 2, it is the schematic diagram of oscillating grinding for crankshaft pin journal, in which O, O' and O'' represent the centers of main journal, grinding wheel and pin journal, respectively; a fixed coordinate system $O-XY$ is attached at O; α is the rotation angle of crankshaft (i.e. C-axis), which satisfies $0 \le \alpha \le 360°$, and the positive direction of α is counterclockwise; P is the grinding point, and P' is the original grinding point when $\alpha = 0$; α_s and L express the variation angle and variation trajectory of grinding point, and the positive direction of α_s is counterclockwise; $\beta = \alpha_s - \alpha$, which satisfies $\beta \ge 0$ when $0 \le \alpha \le 180°$, and $\beta \le 0$ when $180° \le \alpha \le 360°$. Moreover, OO'' is the eccentricity of crankshaft, which equals to r_q; $O'P$ is the radius of grinding wheel, which equals to r_s; $O''P$ is the radius of pin journal, which equals to r_w; OO' represents the displacement of grinding carriage-axis (i.e. X-axis), which equals to x; n_w and n_s represent the average rotation velocities of crankshaft and grinding wheel, respectively. Besides these variables, v_x, a_x and J_x represent the velocity, acceleration and jerk of X-axis, respectively; ω, a_ω and J_ω represent the instantaneous angular velocity, acceleration and jerk of C-axis, respectively; ω_s is the variation velocity of α_s. All these symbols will be used in the rest of the paper.

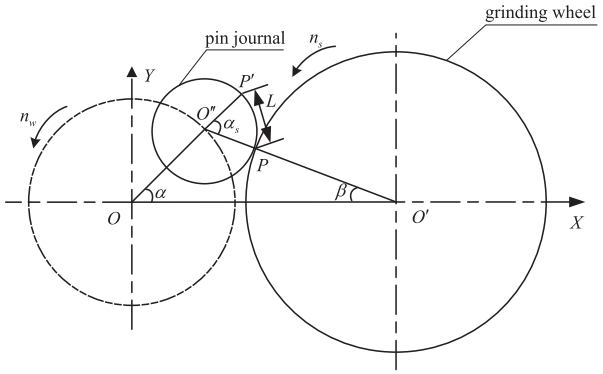

FIGURE 2. The schematic diagram of oscillating grinding.

As mentioned above, the grinding wheel is always tangent with the pin journal during the oscillating grinding process through the linkage between X-axis and C-axis. In fact, the motion model is used to determine the displacement of X-axis (i.e. x) and the instantaneous angular velocity of C-axis (i.e. ω).

In $\Delta O''OO'$ of Fig. 2, by using cosine law, the following geometrical relations of oscillating grinding can be obtained:

$$x^2 = {r_q}^2 + (r_w + r_s)^2 - 2r_q\,(r_w + r_s)\cos(\pi - \alpha_s) \quad (1)$$

$$(r_s + r_w)^2 = x^2 + {r_q}^2 - 2r_q x\cos\alpha \quad (2)$$

Then, let Δt be a time interval, and a time series t_i can be obtained in $\left[0\ \ 1/n_w\right]$, as:

$$\begin{cases} t_1 = 0 \\ t_{i+1} - t_i = \Delta t \\ t_m = \dfrac{1}{n_w} \end{cases} \quad (3)$$

where $1 \le i \le m$.

The displacement x_i can be further calculated combing with (1) and (2) when α or α_s is determined, as:

$$x_i = r_q \cos\alpha_i + \sqrt{(r_s + r_w)^2 - \left(r_q \sin\alpha_i\right)^2} \tag{4}$$

or

$$x_i = \sqrt{{r_q}^2 + (r_w + r_s)^2 - 2r_q\,(r_w + r_s)\cos\left(\pi - \alpha_{si}\right)} \tag{5}$$

Next, the variables of velocity can be obtained through the difference method, as:

$$v_i = \lim_{\Delta t \to 0} \frac{x_{i+1} - x_i}{\Delta t} \tag{6}$$

$$\omega_i = \lim_{\Delta t \to 0} \frac{\alpha_{i+1} - \alpha_i}{\Delta t} \tag{7}$$

$$\omega_{si} = \lim_{\Delta t \to 0} \frac{\alpha_{si+1} - \alpha_{si}}{\Delta t} \tag{8}$$

In the same way, the variables of acceleration and jerk can also be calculated.

B. VELOCITY CHARACTERISTICS AT GRINDING POINT

Generally, equivalent grinding thickness and grinding force are considered as the parameters which heavily affect the grinding quality, and these two parameters are all determined by the velocity at grinding point. Thus, the velocity characteristics at grinding point are analyzed in this subsection.

As shown in Fig. 3, it is the schematic diagram of velocity at grinding point, and a coordinate system $P - mt$ is established at the grinding point. The direction of Pm-axis is pointed from P to O', which represents the normal direction at grinding point; the Pt-axis satisfies the right hand rule with Pm-axis, which represents the tangential direction at grinding point; v_s is the linear velocity of grinding wheel; v_w is the linear velocity of pin journal at grinding point.

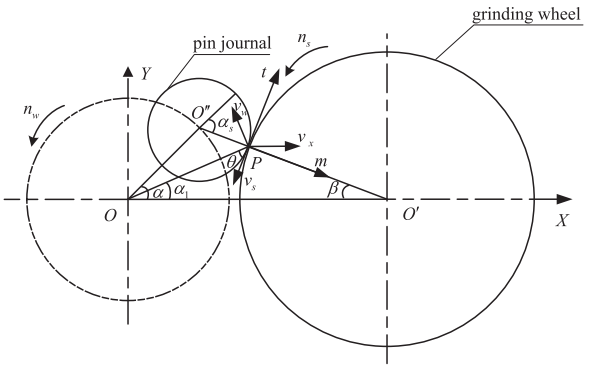

FIGURE 3. The schematic diagram of velocity at grinding point.

First, let v_x and v_s be decomposed to Pt-axis and Pm-axis, respectively, and the following relations can be obtained:

$$v_{t1} = v_x \sin\beta - v_s \tag{9}$$

$$v_{m1} = v_x \cos\beta \tag{10}$$

where v_{t1} and v_{m1} are the tangential velocity and normal velocity of grinding wheel at grinding point, respectively.

Similarly, let v_w be decomposed to Pt-axis and Pm-axis, and the following relations can be obtained:

$$v_{t2} = v_w \sin\theta \tag{11}$$

$$v_{m2} = -v_w \cos\theta \tag{12}$$

where v_{t2} and v_{m2} are the tangential velocity and normal velocity of pin journal at grinding point; θ is the angle between OP and tp, as shown in Fig. 3.

Then, v_w can be expressed as:

$$v_w = \omega\rho \tag{13}$$

where ρ is the length of OP, which can be calculated as:

$$\rho = \sqrt{(r_s \sin\beta)^2 + (x - r_s \cos\beta)^2} \tag{14}$$

On the other hand, θ can be expressed as:

$$\theta = \frac{\pi}{2} - \alpha_1 - \beta \tag{15}$$

where α_1 is the angle between OP and OX, as shown in Fig. 3.

Based on (15), the following relations can be obtained:

$$\sin\theta = \cos\left(\alpha_1 + \beta\right) = \cos\alpha_1 \cos\beta - \sin\alpha_1 \sin\beta \tag{16}$$

$$\cos\theta = \sin\left(\alpha_1 + \beta\right) = \sin\alpha_1 \cos\beta + \cos\alpha_1 \sin\beta \tag{17}$$

In $\Delta POO'$ of Fig. 3, by using sine and cosine laws, $\sin\alpha_1$ and $\cos\alpha_1$ can be expressed as:

$$\sin\alpha_1 = \frac{r_s \sin\beta}{\rho} \tag{18}$$

$$\cos\alpha_1 = \frac{x^2 + \rho^2 - {r_s}^2}{2x\rho} \tag{19}$$

Substituting (14)-(19) to (13), v_w can be calculated.

Through (9)-(12), the resultant velocities at grinding point can be expressed as:

$$v_t = v_{t1} + v_{t2} \tag{20}$$

$$v_m = v_{m1} + v_{m2} \tag{21}$$

where v_t and v_m represent the tangential velocity and normal velocity at grinding point, respectively. In fact, the equivalent grinding thickness and the grinding force are mainly determined by v_{t2}/v_{t1}.

The velocity characteristics analysis can be completed by using (20) and (21) with a certain oscillating grinding motion model. In addition, because the equivalent grinding thickness and the grinding force are mainly determined by the tangential velocity at grinding point, the tangential velocity should be paid more attention.

C. PERFORMANCE OF DRIVING AXIS

The oscillating grinding motion model determines the velocity, acceleration and jerk of each driving axis, and further affects the tracking performance of each driving axis. Thus, in this subsection, the performance analysis of driving axis will be given.

The velocities, accelerations and jerks of X-axis and C-axis can be calculated through the difference method;

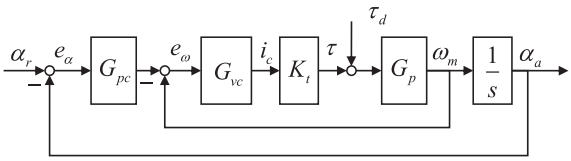

FIGURE 4. The control block diagram of *C*-axis.

then, the servo control system of the driving axis should be established. Taking C-axis as an example, the control system is shown in Fig. 4, and it should be pointed out that compared with displacement and velocity signals, the response of current is much faster, thus, the current loop is equivalent to 1. In this figure, α_r is the reference angular displacement; α_a is the actual angular displacement measured by encoder; e_α and e_ω are the tracking error and angular velocity error, respectively; i_c and ω_m are the driving current and angular velocity of the servo motor, respectively; K_t is the torque coefficient; τ_d represents the disturbance. G_{pc}, G_{vc} and G_p represent the position loop controller, velocity loop controller and control object, respectively, which can be expressed as:

$$G_{pc} = K_{pp} \tag{22}$$

$$G_{vc} = \frac{K_{pv}\left(1 + T_{iv}s\right)}{T_{iv}s} \tag{23}$$

$$G_p = \frac{1}{Js} \tag{24}$$

where K_{pp} is the proportional gain of the position loop controller; K_{pv} and T_{iv} are the proportional gain and integral time constant of the velocity loop controller, respectively; J is the load inertia of C-axis; s is the Laplace operator.

Without considering the disturbance, the tracking error e_α can be written as:

$$e_\alpha = \frac{1 + G_{vc}K_tG_p}{1 + G_{pc}G_{vc}K_tG_p\frac{1}{s} + G_{vc}K_tG_p}\alpha_r \tag{25}$$

Combining (25) with (22), (23) and (24), e_α can be further written as:

$$e_\alpha = \frac{b_1s^3 + b_2s^2 + b_3s}{b_1s^3 + b_2s^2 + b_4s + b_5}\alpha_r \tag{26}$$

where $b_1 = JT_{iv}$, $b_2 = K_{pv}T_{iv}K_t$, $b_3 = K_{pv}K_t$, $b_4 = \left(K_{pp}K_{pv}T_{iv} + K_{pv}\right)K_t$, $b_5 = K_{pp}K_{pv}K_t$.

In actual application, the effective components of α_r always locate in the low frequency region, which means $|s| < s_1$, and s_1 is the upper bound of $|s|$. s_1 is generally sufficient small, and the following relation can be obtained:

$$b_1s^3 + b_2s^2 + b_4s + b_5 \approx b_5 = K_{pp}K_{pv}K_t \tag{27}$$

Thus, (26) can be rewritten as:

$$e_\alpha = \frac{JT_{iv}s^3 + K_{pv}T_{iv}K_ts^2 + K_{pv}K_ts}{K_{pp}K_{pv}K_t}\alpha_r \tag{28}$$

By using inverse Laplace transformation, e_α can be expressed in time domain, as:

$$e_\alpha = \frac{JT_{iv}}{K_{pp}K_{pv}K_t}\dddot{\alpha}_r + \frac{T_{iv}}{K_{pp}}\ddot{\alpha}_r + \frac{1}{K_{pp}}\dot{\alpha}_r \tag{29}$$

Based on (29), the tracking error of driving axis can be calculated combining with the motion parameters. In practice, the grinding accuracy is heavily affected by the tracking error of driving axis. On the other hand, the NC system will be unstable when the tracking error is too large.

Up to now, the velocity characteristics at grinding point and the performance of driving axis have been analyzed, and a complete analysis flow of oscillating grinding motion model is given as follows:

1) Establish an oscillating grinding motion model, and calculate the displacement, velocity, acceleration and jerk of each driving axis;
2) Complete the velocity characteristics analysis at grinding point, including the tangential velocity and the normal velocity;
3) Obtain the tracking error of each driving axis by using (29);
4) Evaluate the oscillating grinding motion model combing the results in 2) and 3); then, select a motion model with stronger practicality.

III. NUMERICAL COMPARISON EXAMPLE

In this section, two oscillating grinding motion models are firstly established; then, a numerical comparison example is given based on the proposed analysis method.

A. ESTABLISHMENT OF OSCILLATING GRINDING MOTION MODELS

The constant liner velocity motion model (CLVMM) and the constant angular velocity motion model (CAVMM) are established in this subsection, which are the two main oscillating grinding motion models.

CLVMM means that the variation of grinding point P on the contour curve is uniform, and the following relation can be obtained:

$$\frac{dL}{dt} = r_w\frac{d\alpha_s}{dt} = C_v \tag{30}$$

where C_v is a constant.

Next, α_s can be expressed as:

$$\alpha_s = \frac{C_v}{r_w}t + \frac{C_1}{r_w} \tag{31}$$

where C_1 is another constant.

Considering that when $t = 0\left(1/n_w\right)$, $\alpha_s = 0\left(2\pi\right)$, then, α_s can be expressed as:

$$\alpha_s = 2n_w\pi t \tag{32}$$

Combining (32) with (5), the displacement x_i can be obtained.

Then, α_i can be calculated as:

$$\begin{cases} \alpha_i = \cos^{-1}\dfrac{{x_i}^2 + {r_q}^2 - (r_s + r_w)^2}{2r_qx_i}\left(t_i \le \dfrac{t_m}{2}\right) \\ \alpha_i = 2\pi - \cos^{-1}\dfrac{{x_i}^2 + {r_q}^2 - (r_s + r_w)^2}{2r_qx_i}\left(\dfrac{t_m}{2} \le t_i \le t_m\right) \end{cases} \tag{33}$$

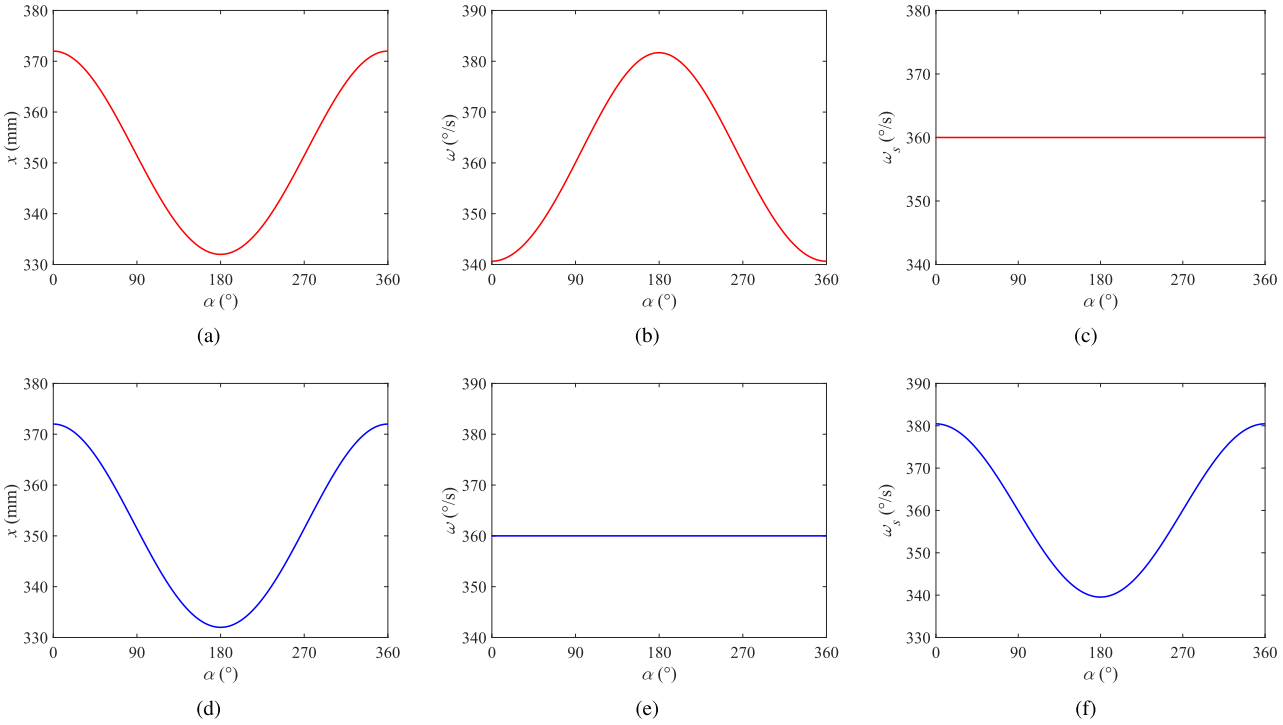

FIGURE 5. x, ω and ω_S with different motion models. (a) x with the CLVMM. (b) ω with the CLVMM. (c) ω_S with the CLVMM. (d) x with the CAVMM. (e) ω with the CAVMM. (f) ω_S with the CAVMM.

CAVMM means that the grinding point has constant angular velocity with respect to $O-XY$, which indicates that ω always equals to n_w during the grinding process, and the following relation can be obtained:

$$\alpha = 2\pi n_w t \tag{34}$$

Combining (34) with (4), the displacement x_i can be obtained. Then, α_s can be calculated as:

$$\begin{cases} \alpha_{si} = \cos^{-1}\dfrac{x_i^2 - r_q^2 - (r_w + r_s)^2}{2r_q(r_w + r_s)} \left(t_i \le \dfrac{t_m}{2}\right) \\ \alpha_{si} = 2\pi - \cos^{-1}\dfrac{x_i^2 - r_q^2 - (r_w + r_s)^2}{2r_q(r_w + r_s)} \left(\dfrac{t_m}{2} < t_i \le t_m\right) \end{cases} \tag{35}$$

It should be pointed out that no matter which motion model is used, the variables of velocity, acceleration and jerk can be obtained by using the difference method, such as (6), (7) and (8).

B. COMPARISON ANALYSIS RESULTS OF MOTION MODELS

In this subsection, a numerical comparison example is performed, and the detailed parameters are given as:

$$\begin{cases} r_q = 20\text{mm} \\ r_w = 22\text{mm} \\ r_s = 330\text{mm} \\ n_w = 60\text{rpm} \\ \Delta t = 0.001\text{s} \\ v_s = 120\text{m/s} \end{cases} \tag{36}$$

Taking α as the independent variable, x, ω and ω_s are given with different motion models, and the results are shown in Fig. 5.

It can be seen clearly that no matter which motion model is used, x is constantly changing during the grinding process; next, ω is changeable when using the CLVMM, and becomes constant when using the CAVMM; on the contrary, ω_s is constant when using the CLVMM, and becomes changeable when using the CAVMM. These results indicate that compared with the CAVMM, the CLVMM requires both X-axis and C-axis move with variable velocities to ensure the uniform variation of grinding point.

Then, the velocity characteristics at grinding point with different motion models are analyzed, and the tangential velocities at grinding point with different motion models are shown in Fig. 6.

One may see that v_{t1}, v_{t2} and v_t are almost the same when using the CLVMM and the CAVMM. Thus, the ratio v_{t2}/v_{t1} will be almost the same. Moreover, because v_s is much larger, v_{t1} and v_t almost equal to 120m/s, and the fluctuation is less than 0.3m/s.

The normal velocities at grinding point with different motion models are further given, as shown in Fig. 7.

Be similar to the tangential velocities, the normal velocities at grinding point are almost the same when using the CLVMM and the CAVMM, the difference is very small. In addition, the maximum amplitude of normal velocity is less than 0.3m/s, which is much less than the tangential velocity.

The analysis results of velocity characteristics indicate that the velocities at grinding point are almost the same when using the CLVMM and the CAVMM. In other words,

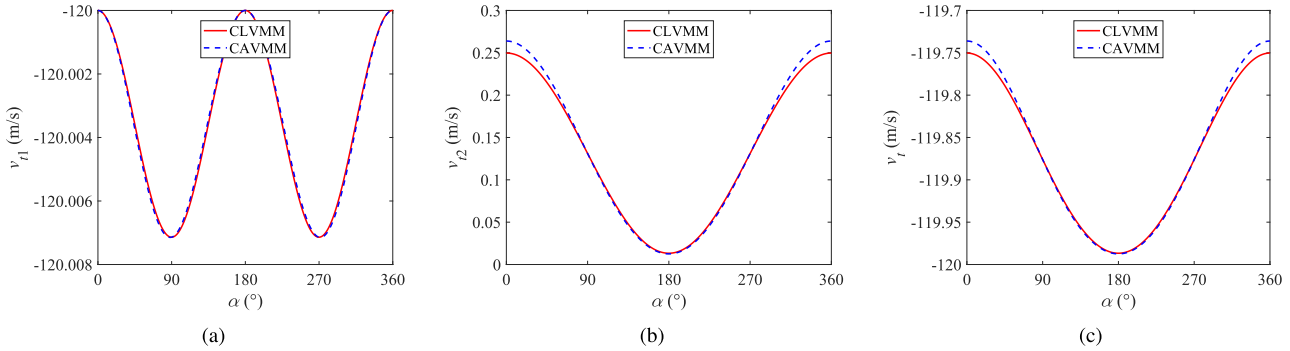

FIGURE 6. The tangential velocities at grinding point with different motion models. (a) v_{t1}. (b) v_{t2}. (c) v_t.

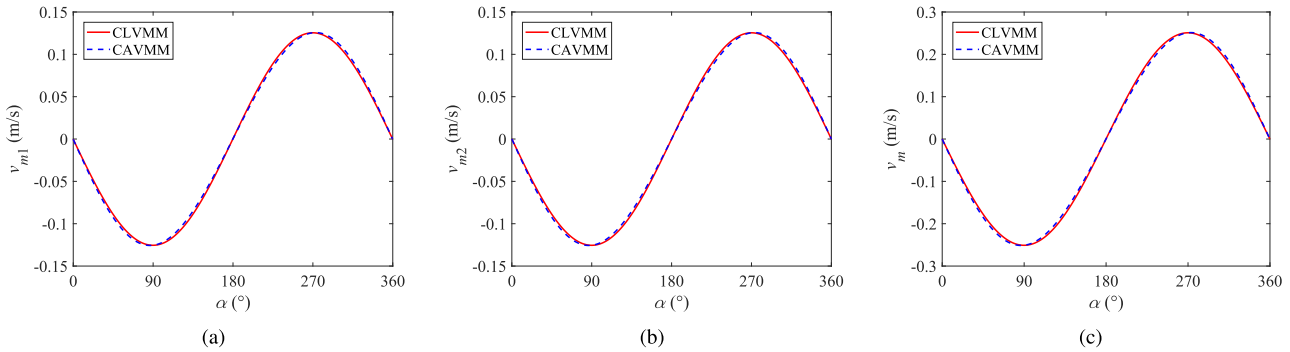

FIGURE 7. The normal velocities at grinding point with different motion models. (a) v_{m1}. (b) v_{m2}. (c) v_m.

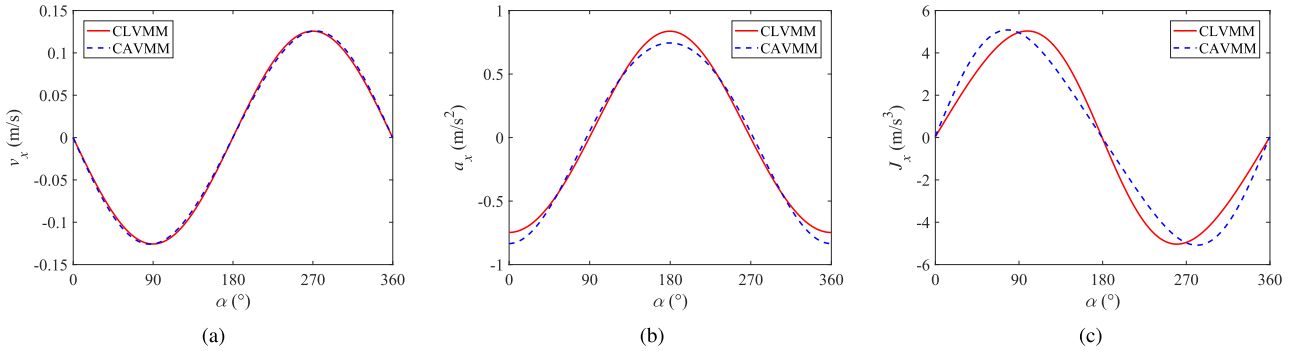

FIGURE 8. The velocity, acceleration and jerk of X-axis with different motion models. (a) Velocity. (b) Acceleration. (c) Jerk.

the CLVMM can only guarantee the uniform variation of grinding point, but cannot guarantee a constant velocity characteristic at grinding point.

Finally, the performance of driving axis is analyzed when using different motion models. The velocity, acceleration and jerk of X-axis are given in Fig. 8. The velocity, acceleration and jerk of X-axis are almost the same when using the CLVMM and the CAVMM, including amplitude and variation trend. The results indicate that these two motion models have the same performance requirement of X-axis.

Furthermore, the velocity, acceleration and jerk of C-axis are given in Fig. 9. It can be seen that when using the CAVMM, the velocity equals to 360°/s, and the acceleration and jerk both equal to 0. On the contrary, when using the CLVMM, the velocity, acceleration and jerk of C-axis are all variable, and the maximum values of acceleration and jerk are more than 100°/s^2 and 1000°/s^3, respectively, which means that compared with the CAVMM, the CLVMM greatly improves the performance requirement of C-axis.

Based on the above results, compared with X-axis, the performance of C-axis (i.e. workpiece rotation-axis) will be huge different when using different motion models, and the tracking error of C-axis is further given to evaluate these two motion models based on (29).

As an numerical example, the tracking error of C-axis is shown in Fig. 10 when K_{pp} = 83.35/s, K_{pv} = 5A·s/rad,

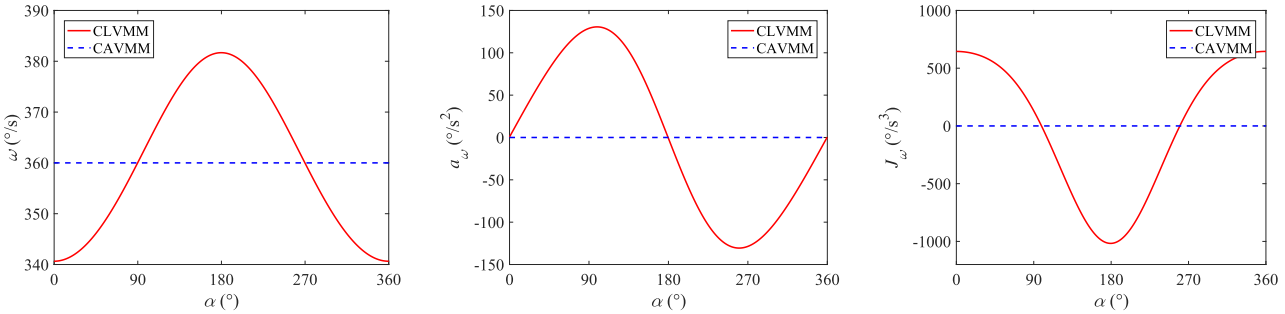

FIGURE 9. The velocity, acceleration and jerk of *C*-axis with different motion models. (a) Velocity. (b) Acceleration. (c) Jerk.

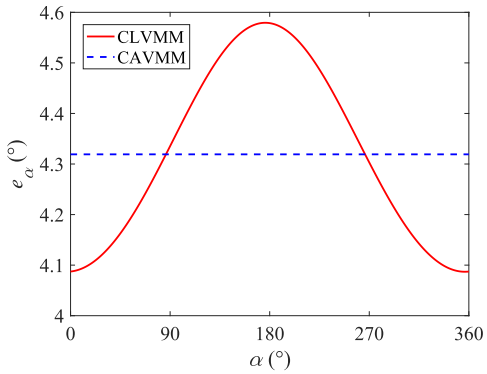

FIGURE 10. The tracking error of *C*-axis with different motion models.

$T_{iv} = 10$ms, $K_t = 1.4$N·m/A, and $J = 0.03$kg·m^2. Obviously, e_α becomes worse when using the CLVMM, which will affect the rotation accuracy of workpiece, and further decrease the grinding quality. On the other hand, the tracking error of C-axis is constant when using the CAVMM, which is easier to compensate than the variable tracking error when using the CLVMM.

Based on the proposed method, the CLVMM and the CAVMM are both analyzed, including the velocity characteristics at grinding point and the performance of driving axis, and the main results are summarized in Table 1.

TABLE 1. Analysis results between the CLVMM and the CAVMM.

Object	CLVMM	CAVMM
Velocity at grinding point	Almost the same as the CAVMM	Almost the same as the CLVMM
Performance of X-axis	Almost the same as the CAVMM	Almost the same as the CLVMM
Performance of C-axis	Worse	Better

The results show that compared with the CAVMM, the CLVMM only guarantees the uniform variation of grinding point, however, the velocities at grinding point are almost the same with these two motion models. Furthermore, the tracking performance of C-axis will decrease when using the CLVMM, which would heavily affect the grinding quality of pin journal. Overall, the CAVMM is more practical than the CLVMM in theory, and an experiment validation will be carried out in next section.

IV. CRANKSHAFT PIN JOURNAL GRINDING EXPERIMENT

In this section, a crankshaft pin journal grinding experiment is performed to validate the effectiveness of the proposed analysis method of oscillating grinding motion model. As shown in Fig. 11, it is the prototype of an oscillating grinding machine tool with two grinding carriages, which is developed by Beier Machine Tool Works Co., LTD. The main technical indices of the oscillating grinding machine tool are listed in Table 2.

TABLE 2. The main technical indices of the oscillating grinding machine tool.

Object	Value
Maximum rotation diameter	520mm
Distance between centers	600/1200mm
Height of center	350mm
Maximum mass of workpiece	150kg
Number of CNC axes	7
Maximum Grinding wheel diameter	Φ 650mm
Maximum linear velocity of CBN grinding wheel	120m/s

The workpiece is shown in Fig. 12, which is a crankshaft with four cylinders. There are totally four pin journals, i.e. P1, P2, P3 and P4 in this figure, and the grinding requirements are given as: 1) the roundness error should be less than 8um; 2) the surface roughness should be less than 0.4um. The main machining parameters are given in Table 3.

TABLE 3. The main machining parameters of crankshaft pin journal grinding experiment.

Object	Description
Grinding cycle mode	Coarse grinding→semi fine grinding→fine grinding
Grinding allowance	0.15mm→0.05mm→0.005mm
Rotation velocity of crankshaft	30rpm in the whole process
Linear velocity of CBN grinding wheel	100m/s in the whole process

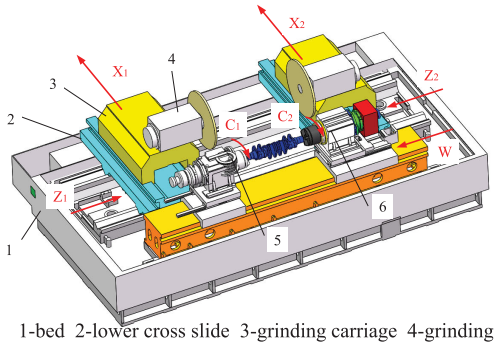

1-bed 2-lower cross slide 3-grinding carriage 4-grinding wheel spindle 5-headstock 6-tailstock

(a)

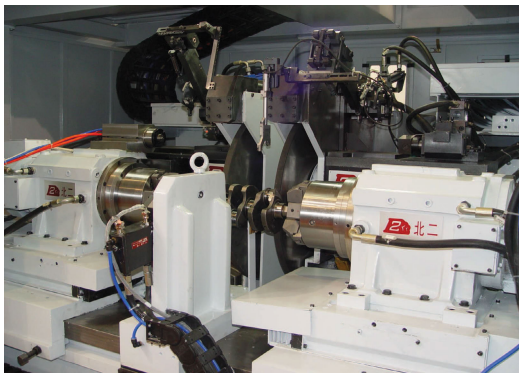

(b)

FIGURE 11. The oscillating grinding machine tool with two grinding carriages. (a) The 3D model. (b) The prototype.

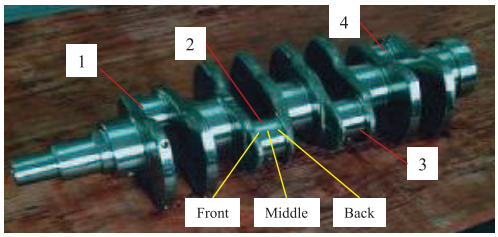

1-pin journal P1 2-pin journal P2 3-pin journal P3 4-pin journal P4

FIGURE 12. The crankshaft workpiece with four cylinders.

First, the CLVMM is tried to complete the grinding of pin journals. However, due to the large tracking error of C-axis, the NC system alarms, and the experiment fails. It should be pointed out that, if the engineers want to use this motion model, much more efforts should be carried out to improve the servo tracking capability of C-axis, which represents more workload and cost.

Next, the CAVMM is used to machining the pin journals, and the experiment is normally completed. Then, the roundness error and surface roughness of each pin journal are detected through corresponding instruments. Because the pin journal has a certain length along the axis-direction of crankshaft, the roundness errors of front, middle and back parts of each pin journal are measured to ensure that the detection results can truly reflect the machining quality of pin journals, as shown in Fig. 12. The detailed detection results are given in Fig. 13. It can be seen clearly that the largest roundness error is less than 6um, and the largest surface roughness is less than 0.32um, which means that the grinding results of all pin journals are qualified.

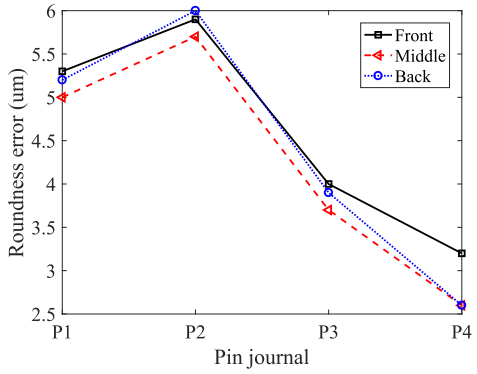

(a)

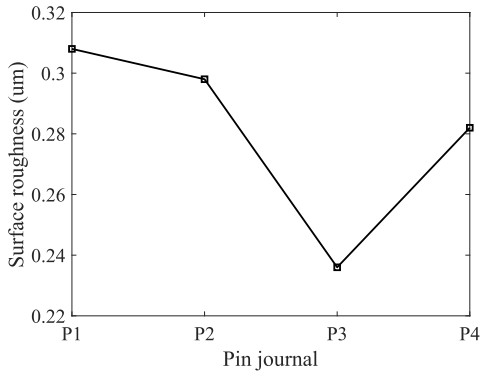

(b)

FIGURE 13. The detection results of pin journals. (a) Roundness errorl. (b) Surface roughness.

The CLVMM and the CAVMM are the two main oscillating grinding motion models, thus, the crankshaft pin journal grinding experiments are performed based on these two models. The results indicate that compared with the CLVMM, the CAVMM is much more practical in industry, which is consistent with theory analysis. Thus, the proposed analysis method of oscillating grinding motion model is effective, and it can also be applied to other oscillating grinding motion models.

In addition, compared with the CAVMM, the only advantage of the CLVMM is the uniform variation of grinding point. The difference of α_s is also given when using these two motion models. α_s can be calculated through (32) when using the CLVMM; then, α_s can also be obtained based on (4) and (35) when using the CAVMM, as:

$$\begin{cases} \alpha_{si} = \cos^{-1} \dfrac{\cos\alpha_i A_r - r_q \sin^2\alpha_i}{(r_w + r_s)} \ (0^\circ \le \alpha_i \le 180^\circ) \\ \alpha_{si} = 2\pi - \cos^{-1} \dfrac{\cos\alpha_i A_r - r_q \sin^2\alpha_i}{(r_w + r_s)} \ (180^\circ \le \alpha_i \le 360^\circ) \end{cases} \tag{37}$$

where $A_r = \sqrt{(r_s + r_w)^2 - (r_q \sin\alpha_i)^2}$.

Let (37) subtract (32), and the following relation can be obtained:

$$\begin{cases} \Delta\alpha_{si} = \cos^{-1}\frac{\cos\alpha_i A_r - r_q \sin^2\alpha_i}{(r_w + r_s)} - 2n_w\pi t_i \\ \qquad (0^\circ \le \alpha_i \le 180^\circ) \\ \Delta\alpha_{si} = 2\pi - \cos^{-1}\frac{\cos\alpha_i A_r - r_q \sin^2\alpha_i}{(r_w + r_s)} - 2n_w\pi t_i \\ \qquad (180^\circ \le \alpha_i \le 360^\circ) \end{cases} \tag{38}$$

where $\Delta\alpha_{si}$ represents the difference of α_s between the CAVMM and the CLVMM.

The results of $\Delta\alpha_s$ are shown in Fig. 14 when $(r_w + r_s)$ equals to different values, and other parameters are the same as shown in (36). One may see that $\Delta\alpha_s$ becomes smaller with the increase of $(r_w + r_s)$, which indicates that it is better to use a grinding wheel with large radius when using the CAVMM in practice to improve the variation uniformity of grinding point.

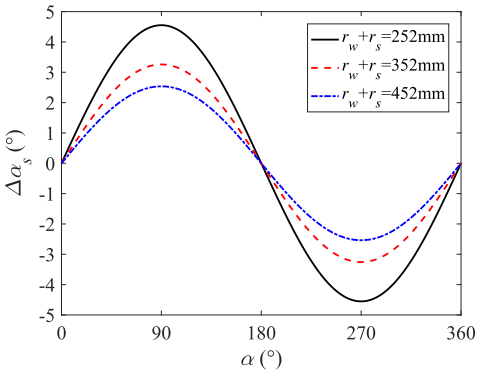

FIGURE 14. $\Delta\alpha_s$ when $(r_w + r_s)$ equals to different values.

V. CONCLUSION

This paper investigates a complete analysis method of oscillating grinding motion model for crankshaft pin journal, involving both theory and experiment. First, the characteristics analysis of oscillating grinding is performed, including the velocity characteristics at grinding point and the performance of driving axis. Then, based on the proposed method, a numerical comparison example is given between the constant linear velocity motion model (CLVMM) and the constant angular velocity motion model (CAVMM). The theory analysis results show that although the CLVMM can guarantee the uniform variation of grinding point, the velocity characteristics at grinding point of these two motion models are almost the same; moreover, the CLVMM will decrease the performance of C-axis in a large extent. Thus, the CAVMM is more practical than the CLVMM in theory. Finally, a crankshaft pin journal grinding experiment is performed on a prototype, and the result also indicates that the CAVMM is more practical, which is consistent with the theory analysis and validates the effectiveness of the proposed analysis method. A suggestion of improving the variation uniformity of grinding point is also given when using the CAVMM. Moreover, the proposed analysis method can also be applied to other motion models.

REFERENCES

[1] J. F. G. Oliveira, E. J. Silva, C. Guo, and F. Hashimoto, "Industrial challenges in grinding," *CIRP Ann.*, vol. 58, no. 2, pp. 663–680, 2009.
[2] H. K. Tönshoff, B. Karpuschewski, T. Mandrysch, and I. Inasaki, "Grinding process achievements and their consequences on machine tools challenges and opportunities," *CIRP Ann.*, vol. 47, no. 2, pp. 651–668, 1998.
[3] M. Hitchiner and J. Webster, "Recent advances in camshaft and crankshaft grinding," *Abrasives*, pp. 8–12, 2001.
[4] T. Fujiwara, S. Tsukamoto, and M. Miyagawa, "Analysis of the grinding mechanism with wheel head oscillating type CNC crankshaft pin grinder," *Key Eng. Mat.*, vols. 291–292, pp. 163–170, Aug. 2005.
[5] *Generator SS Crankshaft*. Accessed: Aug. 8, 2019. [Online]. Available: https://www.indiamart.com/proddetail/generator-ss-crankshaft-15725979288.html
[6] M. Zhang and Z. Yao, "Force characteristics in continuous path controlled crankpin grinding," *Chin. J. Mech. Eng.*, vol. 28, no. 2, pp. 331–337, Mar. 2015.
[7] Z. Jiang and Y. He, "Research on stability prediction of the crankshaft CNC tangential point tracing grinding," *Math Problems Eng.*, vol. 2015, Sep. 2015, Art. no. 106159.
[8] B. Denkena and O. Gümmer, "Active tailstock for precise alignment of precision forged crankshafts during grinding," *Proc. CIRP*, vol. 12, pp. 121–126, 2013.
[9] H.-C. Möhring, O. Gümmer, and R. Fischer, "Active error compensation in contour-controlled grinding," *CIRP Ann.*, vol. 60, no. 1, pp. 429–432, 2011.
[10] A. P. Walsh, B. Baliga, and P. D. Hodgson, "Force modelling of the crankshaft pin grinding process," *Proc. Inst. Mech. Eng., D, J. Automobile Eng.*, vol. 218, no. D3, pp. 219–227, Mar. 2004.
[11] H. Yu, M. Xu, and J. Zhao, "In-situ roundness measurement and correction for pin journals in oscillating grinding machines," *Mech. Syst. Signal Process.*, vols. 50–51, pp. 548–562, Jan. 2015.
[12] K. C. Cha, N. Wang, and J. Y. Liao, "Stability analysis for the crankshaft grinding machine subjected to a variable-position worktable," *Int. J. Adv. Manuf. Technol.*, vol. 67, nos. 1–4, pp. 501–516, Jul. 2013.
[13] P. Krajnik, R. Drazumeric, and J. Badger, "Optimization of peripheral non-round cylindrical grinding via an adaptable constant-temperature process," *CIRP Ann.*, vol. 62, no. 1, pp. 347–350, 2013.
[14] R. Drazumeric, J. Badger, and P. Krajnik, "Geometric, kinematical and thermal analyses of non-round cylindrical grinding," *J. Mater. Process Tech.*, vol. 214, no. 4, pp. 818–827, Apr. 2014.
[15] P. Comley, I. Walton, T. Jin, and D. J. Stephenson, "A high material removal rate grinding process for the production of automotive crankshafts," *CIRP Ann.*, vol. 55, no. 1, pp. 347–350, 2006.
[16] T. Torims, J. Vilcans, M. Zarins, A. Avisane, and R. Moksins, "New approach for the crankshafts grinding and determination of the 3D surface roughness model for the crankshafts bearings," *Ann. DAAAM*, vol. 20, no. 1, pp. 1563–1565, 2009.
[17] D. C. Fricker, T. R. A. Pearce, and A. J. L. Harrison, "Predicting the occurrence of grind hardening in cubic boron nitride grinding of crankshaft steel," *Proc. Inst. Mech. Eng., B, J. Eng. Manuf.*, vol. 218, no. 10, pp. 1339–1356, Oct. 2004.
[18] Y. Liu, J. Fan, and W. Miao, "Soft compensation for CNC crankshaft grinding machine tool," *Adv. Mech. Eng.*, vol. 5, 2013, Art. no. 254709.
[19] W. Wei and G. Zhang, "Tool path modeling and error sensitivity analysis of crankshaft pin CNC grinding," *Int. J. Adv. Manuf. Tech.*, vol. 86, nos. 9–12, pp. 2485–2502, Oct. 2016.
[20] B.-L. Jian, C.-C. Wang, J.-Y. Chang, X.-Y. Su, and H.-T. Yau, "Machine tool chatter identification based on dynamic errors of different self-synchronized chaotic systems of various fractional orders," *IEEE Access*, vol. 7, pp. 67278–67286, 2019.
[21] Y. Yong, Z. Wei-Min, Z. Qi-Xin, and J. Quan-Sheng, "Dynamic characteristic optimization of ball screw feed drive in machine tool based on modal extraction of state space model," *IEEE Access*, vol. 7, pp. 55524–55542, 2019.
[22] Y. Li, X. Zhang, Y. Ran, W. Zhang, and G. Zhang, "Reliability and modal analysis of key meta-action unit for CNC machine tool," *IEEE Access*, vol. 7, pp. 23640–23655, 2019.

LIPING WANG was born in Jilin, China. He received the B.S. degree in computer science and the Ph.D. degree in mechanical engineering from Jilin University, Changchun, China, in 1990 and 1997, respectively.

He is currently a Professor with the Department of Mechanical Engineering, Tsinghua University, Beijing, China. His current research interests include parallel mechanisms, machine tools, and motion simulators.

DONG WANG was born in Yunnan, China. He received the B.S. degree in control engineering from Beihang University, Beijing, China, in 2013, and the Ph.D. degree in mechanical engineering from Tsinghua University, Beijing, in 2018, where he currently holds a postdoctoral position with the Department of Mechanical Engineering.

His research interests include dynamics and control of robotics and machine tools.

BO WANG was born in Beijing, China. He received the B.S. degree in mechanical engineering from the Tianjin Institute of Textile Science and Technology, Tianjin, China, in 1993, and the Ph.D. degree in engineering from Tsinghua University, Beijing, in 2019.

He is currently a Senior Mechanical Engineer. His research interest includes CNC machine tool and related technology.

WEIHUA LI was born in Henan, China. He received the B.S. degree in mechanical engineering from the North China Institute of Aeronautical Industry, Beijing, China, in 1996.

He is currently a Senior Mechanical Engineer. His research interest includes CNC grinding machine tool and related technology.